How Changing the Inversion/Eversion Foot Angle Affects the Nondriving Intersegmental Knee Moments and the Relative Activation of the Vastii Muscles in Cycling

Colin S. Gregersen
Biomedical Engineering Program,
One Shields Avenue,
University of California,
Davis, CA 95616

M. L. Hull
Department of Mechanical Engineering
and Biomedical Engineering Program,
One Shields Avenue,
University of California,
Davis, CA 95616
e-mail: mlhull@ucdavis.edu

Nils A. Hakansson
Biomedical Engineering Program,
One Shields Avenue,
University of California,
Davis, CA 95616

Nondriving intersegmental knee moment components (i.e., varus/valgus and internal/external axial moments) are thought to be primarily responsible for the etiology of overuse knee injuries such as patellofermoral pain syndrome in cycling because of their relationship to muscular imbalances. However the relationship between these moments and muscle activity has not been studied. Thus the four primary objectives of this study were to test whether manipulating the inversion/eversion foot angle alters the varus/valgus knee moment (Objective 1) and axial knee moment (Objective 2) and to determine whether activation patterns of the vastus medialis oblique (VMO), vastus lateralis (VL), and tensor fascia latae (TFL) were affected by changes in the varus/valgus (Objective 3) and axial knee moments (Objective 4). To fulfill these objectives, pedal loads and lower limb kinematic data were collected from 15 subjects who pedaled with five randomly assigned inversion/eversion angles: 10 deg and 5 deg everted and inverted and 0 deg (neutral). A previously described mathematical model was used to compute the nondriving intersegmental knee moments throughout the crank cycle. The excitations of the VMO, VL, and TFL muscles were measured with surface electromyography and the muscle activations were computed. On average, the 10-deg everted position decreased the peak varus moment by 55% and decreased the peak internal axial moment by 53% during the power stroke (crank cycle region where the knee moment is extensor). A correlation analysis revealed that the VMO/VL activation ratio increased significantly and the TFL activation decreased significantly as the varus moment decreased. For both the VMO/VL activation ratio and the TFL activation, a path analysis indicated that the varus/valgus moment was highly correlated to the axial moment but that the correlation between muscle activation and the varus moment was due primarily to the varus/valgus knee moment rather than the axial knee moment. The conclusion from these results is that everting the foot may be beneficial towards either preventing or ameliorating patellofemoral pain syndrome in cycling. [DOI: 10.1115/1.2193543]

Introduction

Overuse injury in cycling is commonly manifest at the knee joint [1–3], where chondromalacia of the patella, or more generally classified as patellofemoral pain syndrome [4,5] is the most common overuse knee injury [1]. One possible cause of patellofemoral pain syndrome has been attributed to a muscular force imbalance between medial and lateral quadriceps muscles, where patellar tracking is affected [6,7]. During the power stroke, when the quadriceps muscles are contracting, patellofemoral contact pressures are maximum [8,9]. Either medial or lateral deviations in patellar tracking during this period could result in abnormally high patellofemoral contact pressures [10–12], which, over thousands of loading cycles, could increase the potential for injury to the patellofemoral articulation.

Patellofemoral pain syndrome could be explained by the relationship between the mechanical loading of the knee during pedaling and the corresponding activity of the muscles crossing the knee joint. One possible cause of patellofemoral overuse injury is a varus knee moment, which is typically developed during the power stroke in cycling [13–16]. The vastus lateralis (VL), having a valgus moment arm in addition to its extensor moment arm [17,18], could resist this applied varus moment. The VL could be preferentially activated over the vastus medialis oblique (VMO), creating a quadriceps imbalance and lateral patellar tracking, which is consistent with lateral patellofemoral pain [19]. Additionally, because the tensor facia latae (TFL) inserts on the patella [19,20] and also has a moment arm that develops a valgus moment [17], the TFL could also resist the varus knee moment during the power stroke, leading to increased lateral patellar tracking.

Another load component that could be related to the action of the muscles crossing the knee is the internal/external axial moment. During the power stroke, the axial moment begins internal and becomes external [16]. It is possible that both the VL and TFL resist an internally applied axial moment as well as a varus moment [20,21]. Again, if these muscles resisted large internal axial moments, then the patella could be drawn laterally.

To examine whether the force production of the vastii muscles and the TFL is related to the varus/valgus knee loading during pedaling, it would be desirable to manipulate the varus/valgus

knee moment. One possibility for manipulating the varus/valgus moment is to change the inversion/eversion angle at which the foot interfaces with the pedal. A trend toward a decrease in varus knee moments has been reported for subjects who exhibited more overall forefoot varus [15]. Accordingly physically manipulating the inversion/eversion foot angle in turn may alter the varus/valgus moment transmitted by the knee. The first objective of this study was to test whether manipulating the inversion/eversion foot angle alters the varus/valgus knee moment in cycling.
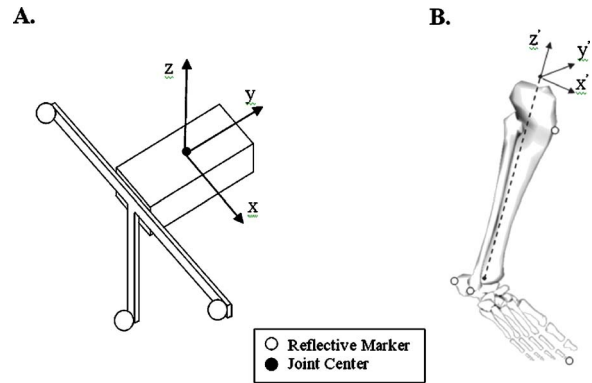
Manipulating the inversion/eversion foot angle may also affect the axial moment transmitted by the knee. Previous studies have shown that a varus/valgus moment applied to the knee causes a coupled axial rotation of the tibia with the respect to the femur [22,23]. Coupled axial moments could be transmitted across the knee if the axial rotations were constrained, as would be the case for a foot-pedal interface that does not allow relative motion between the foot and pedal. The second objective of this study was to test whether manipulating the inversion/eversion foot angle also alters the axial knee moment in cycling. For both the first and second objectives, a related secondary objective was to perform a moment decomposition analysis [14] to understand the mechanism responsible for any changes in both the varus/valgus and axial moments due to changes in the inversion/eversion angle of the foot.

If the inversion/eversion angle affects both the varus/valgus and axial moments, then the activity of the muscles crossing the joint may be related to both moments. The VL could resist both varus and internal axial moments whereas the VMO could resist both valgus and external axial moments. Similar to the VL, the TFL also could resist both varus and internal axial moments. These relationships could be important, where the demands placed on these muscles could be related to both the timing and magnitude of the applied moments. Thus the third and fourth objectives of this study were to determine whether the activation patterns of muscles crossing the knee were related to changes in the varus/valgus (Objective 3) and axial knee moments (Objective 4).

Methods

Analytic Model. A previously described three-dimensional mathematical model was developed to compute the intersegmental knee loads [16]. In brief, an inverse dynamics approach was utilized, where the shank and foot segments were modeled as rigid bodies interconnected by spherical joints and the intersegmental loads were computed at centers of the ankle and knee joints [24]. The model inputs necessary to solve for the intersegmental loads were the segment kinematics, body segment parameters (i.e., masses, moments of inertia, centers of mass locations), and external loading of the foot by the pedal. The three-dimensional segment kinematics were obtained by tracking reflective markers on the pedal, foot, and shank segments. Markers were mounted on the subject's heel, toe, lateral malleolus, medial malleolus, tibial tuberosity, lateral epicondyle, and medial epicondyle. In addition, three markers were mounted on the pedal body (Fig. 1). The heel marker was mounted over the cycling shoe to represent the posteriormost point on the heel. Similarly, the toe marker was mounted to represent the tip of the longest toe (first or second). These markers in conjunction with virtual markers located at the ankle joint center, knee joint center, and the origin of the pedal coordinate system were used to obtain the three-dimensional foot and shank segment kinematics and center of mass locations for the foot and shank segments. The body segment parameters were estimated for each subject [25]. The external loads were measured using a six-load-component pedal dynamometer [26]. All measurements were performed on the right lower extremity.

Knee loads were expressed in a shank-fixed coordinate system (Fig. 1) where the axes reflected the functional axes of the knee joint [27], yet were constrained to remain orthogonal. The z' axis was the line that connected the knee joint center to the ankle joint center. The x' and y' axes were located in a plane perpendicular to the

Fig. 1 (*a*) Diagram illustrating pedal dynamometer reflective markers and local pedal coordinate system. (*b*) Diagram illustrating lower limb reflective markers and virtual joint centers for the ankle and knee joints. The knee joint center served as the origin of the local shank coordinate system in which the knee load components were computed.

the z' axis, where the y' axis was the projection of the knee flexion/extension axis onto this plane (medial direction positive). The x' axis was mutually perpendicular to the other two axes (anterior direction positive). These axes represented the internal/external axial (z'), flexion/extension (y'), and varus/valgus (x') axes of the knee joint. Intersegmental knee loads were expressed as loads applied to the tibia that must be equilibrated by structures crossing the knee (i.e., muscles, ligaments, and bones). This convention can be interpreted as tendencies for relative motion of the tibia with respect to the femur. Hence, a positive My' would act to flex the knee joint (flexor applied moment), a positive Mx' would cause the tibia to adduct relative to the femur (varus applied moment), and a positive Mz' would cause the tibia to rotate internally relative to the femur (internal axial moment).

Experiment. Fifteen competitive cyclists, none of whom had a history of overuse knee injury in cycling, volunteered to participate in the study. The age of the subjects ranged from 18 years to 30 years (mean 28 years), the heights ranged from 1.73 m to 1.91 m (mean 1.82 m), and the weights ranged from 65.8 kg to 95.3 kg (mean 77.7 kg). The subjects pedaled a conventional racing bicycle mounted on an electronically braked Velodyne ergometer (Frontline Technology, Inc., Irvine CA) that allowed a constant workrate to be set independent of pedaling rate. The subjects adjusted the bicycle to match their own bicycle's geometry. The subjects all used clipless pedals, which fixed the foot rigidly without allowing relative motion (i.e., zero float), and chose their own cleat angle.

Surface electrodes were placed over the belly of the vastus lateralis (VL), oblique fibers of the vastus medials (VMO), and belly of the tensor fascia latae (TFL) to record electromyograms (EMG). The electrodes (Motion Lab Systems, Baton Rouge, LA Model MA-300-10) were fit with custom-made silver-silver chloride electrode cups (In Vivo Metric, Healdsburg, CA) and placed according to the recommendations of Delagi et al. [28]. The electrode cups were filled with electrode cream and the electrode was attached to the shaved, abraded skin surface with adhesive washers. Following placement, an adhesive elastic wrap (Vet-wrap, 3M Corporation) was wrapped around the leg to secure the electrode attachment. Following the experiment, resting baseline EMG values were also obtained while the subject rested in a supine position for 5 s. The baseline data were used to subtract any baseline noise present in the EMG records.

The inversion/eversion ankle angle was manipulated by fixing the foot at a constant inversion/eversion angle using a custom-built foot/pedal interface that allowed up to 25 deg of either eversion or inversion (Fig. 2). Additionally, because the ankle joint

Fig. 2 Photograph of six-load-component pedal dynamometer with inversion/eversion interface attached. The interface also has a medial/lateral translational adjustment.

center moves either medially or laterally when the frontal plane foot angle is altered, the interface was also constructed to translate along the medial/lateral direction of the pedal. This feature was used to standardize the distance between the ankle joint center and the crank arm for all frontal plane foot angles. Five foot angle treatments were randomly assigned to each subject, 10 deg inverted (+10), 5 deg inverted (+5), neutral (0), 5 deg everted (−5), and 10 deg everted (−10). All degree measures were relative to the horizontal plane. Rigid-soled road cycling shoes were provided for the subjects (Model SH-R090, Shimano Ltd., Osaka, Japan). To eliminate any possible compensation of the contralateral limb to these treatments as well as match the mass of the measurement limb, a "dummy" pedal and interface were constructed for the contralateral side. The dummy interface allowed the same foot positioning as the measurement limb but the dummy pedal did not measure the loads. The dummy interface was always adjusted to match the foot angles of the measurement limb.

The testing protocol consisted of a 15-min warm-up period at a workrate of 100 W and cadence of 90 rpm for each randomly assigned foot angle treatment. Following the warm-up period, experimental data were recorded while the subject pedaled at a workrate of 225 W and 90 rpm for 5 min in a 52×19 gear. Subjects rested for 10 min between each inversion/eversion treatment to reduce possible carry-over effects and fatigue. Four, 5-sec trials were recorded for each inversion/eversion foot angle setting yielding approximately 30 cycles of data at each treatment. After data collection, all pedal dynamometer and marker path data were filtered using a fourth-order, zero-phase-shift, low-pass Butterworth filter with a cutoff frequency of 6 Hz [29].

Transducer data were collected and processed utilizing a motion capture system (Motion Analysis Inc., Santa Rosa, CA). Four high-speed video cameras recorded the three-dimensional marker positions. Both the dynamometer and EMG outputs were synchronized with and collected by the motion capture system. The camera sampling frequency was 120 Hz, while the sampling frequency of the dynamometer and EMG signals was 1200 Hz.

Data Analysis. Knee load components were computed using the three-dimensional model and were expressed as a function of crank angle where the 0 deg reference was the top-dead-center position (crank arm vertical and upward). The total number of complete cycles for each subject was used to compute average load component curves as a function of crank angle. To obtain these averages for each subject, the load components for all complete pedal revolutions for each subject were linearly interpolated in 5-deg increments of the crank angle. While all six intersegmental knee load components (Fx′, Fy′, Fz′, Mx′, My′, and Mz′) were computed, only the nondriving knee moment components (Mx′ and Mz′) were analyzed further.

To quantify the nondriving moment component curves, five descriptive quantities were computed for each load component. Four of the quantities were the maximum value, minimum value, and angular locations of the maximum and minimum values. The fifth quantity was the average value during the power stroke. For each subject, the power stroke was defined as the region of the crank cycle when the applied driving knee moment was flexor and the recovery stroke was when the applied driving knee moment was extensor.

EMG recordings from all trials, including both baseline and data collection, were full-wave rectified, and filtered with a fourth-order, zero phase-shift Butterworth low-pass digital filter with cut-off frequency of 10 Hz [29]. The records were then normalized to the maximum value measured for the respective muscle during all the pedaling trials. To determine muscle activation $a^m(t)$, the normalized EMG data $u(t)$ were input into a first-order differential equation modeling the activation dynamics as follows [30]:

$$\dot{a}^m = \begin{cases} [u - a^m] \cdot [c_1 u + [c_2 \ldots c_2]^T] & u \geq a^m \\ [u - a^m] \cdot c_2 & u < a^m \end{cases} \quad (1)$$

where $c_1 = \tau_{act}^{-1} - \tau_{deact}^{-1}$, and $c_2 = \tau_{deact}^{-1}$ [31]. The muscle activation and deactivation time constants were 20 ms and 60 ms, respectively [31–33]. The activation was interpolated with cubic splines and expressed in 1-deg increments of the crank cycle. For 6 of the 15 subjects, the EMG recordings for the TFL were not processed due to technical difficulties encountered during the experiment.

Descriptive quantities were computed for the muscle activation versus crank angle curves. Both the peak and average activation during the power stroke were computed for each muscle for all subject-treatment combinations. Because the ratio between VMO and VL activation was of primary interest, the VMO to VL activation ratio (VMO/VL) was computed for both the peak and average values. Because of the intersubject variability common to EMG records, the activation quantities were expressed relative to the neutral case and relative to each subject. Hence, each quantity was expressed as a percent change from the neutral case for each subject. All of the dependent variables were computed on a cycle-by-cycle basis and averaged across cycles for each treatment-subject combination.

To test whether manipulating the inversion/eversion foot angle alters the varus/valgus and axial knee moments, a one-factor repeated measures analysis-of-variance (ANOVA) was utilized to test for significant differences in each of the five quantities used to describe the nondriving moments. In each ANOVA the single independent variable was the inversion-eversion foot angle at five levels (i.e., −10, −5, 0, +5, +10). Because the residual errors within a subject were not likely to be independent between foot angle treatments, the Huynh-Feldt adjusted p value was used as the significance criterion [34]. Additionally, if the Huynh-Feldt p value met the significance criterion ($p < 0.05$), then a polynomial decomposition analysis was performed to test for a linear relation in the response variables across the treatment levels. Significance tests were performed on each term of a fourth-order polynomial. If the null hypothesis (i.e., no curvature) was accepted, then all

Table 1 Repeated measures ANOVA results for the effect of the inversion/eversion foot angle (Huynh-Feldt (H-F) *p* value) on peak nondriving knee moments and angular locations of peak values. Means and contrast tests against the neutral ankle angle (0 deg) are presented. Additionally, the *p* value for the first-order (i.e., linear) term of the polynomial decomposition is presented. Units are Newton-meters for moments and degrees for angles.

	H-F *p* value	10 deg everted	5 deg everted	Neutral	5 deg inverted	10 deg inverted	Linear *p* value
Peak value[b]							
Varus (+Mx′)	<0.0001	3.55	5.14	7.84	9.43	11.53	<0.0001
Valgus (−Mx′)	0.0011	−10.07	−9.13[a]	−8.11	−8.10[a]	−7.68[a]	0.0022
Internal Axial (+Mz′)	<0.0001	0.71	0.75	1.50	2.15	2.82	<0.0001
External Axial (−Mz′)	<0.0001	−3.63	−2.89[a]	−2.50	−2.32[a]	−2.68[a]	0.0028
Peak angle							
Varus (+Mx′)	0.2621	62.3[a]	69.3[a]	67.0	77.0[a]	80.0[a]	N/A[c]
Valgus (−Mx′)	0.1514	212.7[a]	220.0[a]	231.3	231.3[a]	235.3[a]	N/A[c]
Internal Axial (+Mz′)	0.7268	43.3[a]	46.7[a]	27.3	35.3[a]	45.3[a]	N/A[c]
External Axial (−Mz′)	0.0016	102.7[a]	118.3[a]	130.3	151.3[a]	182.3	0.0006

[a]Not significantly different from the neutral foot angle (0 deg) at 0.05 level.
[b]For each subject, the respective maximum value or minimum value was obtained and included in computing the average peak value regardless of sign.
[c]H-F *p* value not significant, hence the polynomial decomposition was not performed.

higher order terms in the polynomial decomposition were not significant ($p > 0.05$) while the linear term was significant ($p < 0.05$).

To understand the mechanism responsible for any changes in both the varus/valgus and axial moments due to eversion of the foot, the moment decomposition analysis was performed [14]. This analysis decomposes each intersegmental knee load component into the individual contributions of five load components at the pedal and inertial contributions. The equations for the varus/valgus (Mx′) and internal/external axial (Mz′) moments are

$$Mx' = Mx'(Fx) + Mx'(Fy) + Mx'(Fz) + Mx'(Mx) + Mx'(Mz)$$
$$+ Mx'(g) \qquad (2)$$

$$Mz' = Mz'(Fx) + Mz'(Fy) + Mz'(Fz) + Mz'(Mx) + Mz'(Mz)$$
$$+ Mz'(g) \qquad (3)$$

where the terms in the equations are the decomposed contributions (i.e., subcomponents) of the pedal forces (Fx, Fy, and Fz), pedal moments (Mx and Mz), and the weight contributions (g).

To determine whether the activation patterns of muscles crossing the knee were related to changes in the varus/valgus and axial knee moments, Pearson's correlation coefficients were calculated between the descriptive quantities of the activation and maximum and average values of the nondriving moments in the power stroke. Because a correlation performed on all subjects for all angles would contain subject-to-subject variability, correlation coefficients were computed between the muscle activation quantities (peaks and averages for the VMO/VL ratio and TFL) and the nondriving moment quantities (peaks and averages) with the mean value removed from all quantities for a given subject. This process removed subject effects from the correlations. Correlation coefficients were computed between four of the nondriving moment quantities (varus peak, internal axial peak, varus/valgus average, and internal/external axial average) and the two muscle activation quantities (peak and average) for the VMO/VL ratio using the complete sample of subjects ($n=15$), and for all subjects with useable TFL records ($n=9$).

Because the varus/valgus and internal/external axial moments were expected to be correlated to each other, it was of interest to determine the respective contributions of each load component to any predictive relationship (i.e., correlation) between the quantities describing the load components and those describing the muscle activation [35]. To accomplish this, a path analysis was

performed in which standardized regression coefficients were computed from a linear regression model using standardized variables (zero mean and unit variance). For this analysis, the muscle activation quantities were the dependent variables and the moment quantities were the independent variables. The regression model was

$$y = b_1 * x_1 + b_2 * x_2 \qquad (4)$$

where y is the muscle activation variable (peak or average), x_1 and x_2 are the respective varus/valgus and internal/external axial variables, and b_1 and b_2 are the standardized regression coefficients. The correlation coefficients obtained between the muscle activation and the moment variables (i.e., $\rho(y,x_1)$ and $\rho(y,x_2)$) were then separated into two components using the equations

$$\rho(y,x_1) = b_1 + \rho(x_1,x_2) * b_2 \qquad (5)$$

$$\rho(y,x_2) = b_2 + \rho(x_1,x_2) * b_1 \qquad (6)$$

where $\rho(x_1,x_2)$ is the correlation coefficient between the two independent variables. The first component of the right side of these equations is the direct effect of one independent variable on y while the second component is the indirect effect of the other independent variable on y. Path diagrams were constructed to illustrate these results where the standardized coefficients reflect the relative contributions of each load component variable to the muscle activation variable of interest. The path analysis was performed for the complete sample of subjects for the VMO/VL ratio ($n=15$), and for all subjects with useable TFL records ($n=9$) when correlation coefficients between muscle activation variables and non-driving moment variables were statistically significant.

Results

Nondriving Knee Moments and Foot Angle. Both the peak varus knee moment and the average value of the varus/valgus moment developed during the power stroke decreased significantly from the neutral condition when the foot was everted and increased significantly when the foot was inverted ($p < 0.0001$) (Tables 1 and 2, Fig. 3). Averaged over all of the subjects, the 10-deg everted angle reduced the peak varus moment by 4.29 Nm (55% of neutral) while the 10-deg inverted angle increased the peak varus moment by 3.69 Nm (47% of neutral) (Table 1). The average varus/valgus moment was varus at the neutral condition and decreased by 3.21 Nm (279% of neutral) becoming valgus for

Table 2 Repeated measures ANOVA results for the effect of the inversion/eversion foot angle (Huynh-Feldt (H-F) *p* value) on average values of the varus/valgus and internal/external axial knee moments during the power stroke. Means and contrast tests against the neutral ankle angle (0 deg) are presented. All contrasts were significant at the 0.05 level. Additionally, the *p* value for the first-order (i.e., linear) term of the polynomial decomposition is presented. Units are Newton-meters.
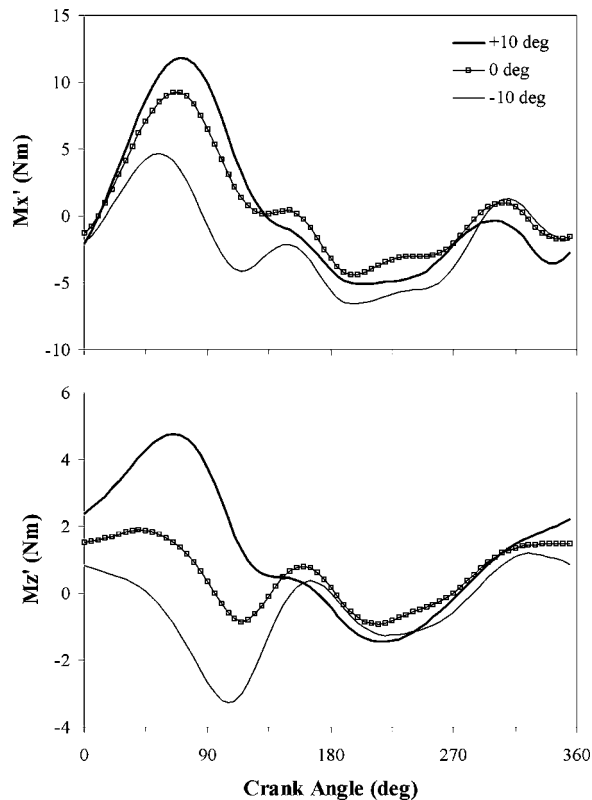
Moment	H-F *p* value	10 deg everted	5 deg everted	Neutral	5 deg inverted	10 deg inverted	Linear *p* value
Varus(+)/Valgus(−)	<0.0001	−2.06	−0.68	1.15	2.15	3.21	<0.0001
Internal(+)/ External(−) Axial	<0.0001	−1.12	−0.57	0.27	0.85	1.32	<0.0001

the 10-deg everted angle and increased by 2.06 Nm (179% of neutral) becoming more varus for the 10-deg inverted angle (Table 2). The polynomial decomposition indicated that both peak varus and average varus/valgus moment values were linearly related to the foot angle ($p < 0.0001$). The angular locations of the peak varus moment occurred near 70 deg and were not affected by the foot angle ($p = 0.2621$) (Table 1).
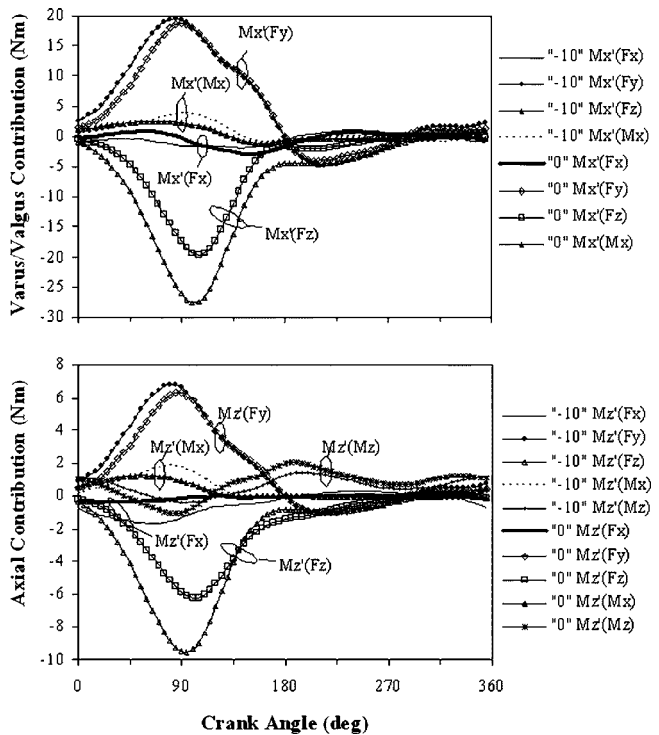
Both the peak internal axial moment and the average value of the internal/external axial moment developed during the power stroke decreased when the foot was everted and increased when the foot was inverted ($p < 0.0001$) (Tables 1 and 2, Fig. 3). Averaged over all of the subjects, the peak internal axial moment significantly decreased by 0.79 Nm (53% of neutral) when the foot was 10-deg everted and increased by 1.32 Nm (88% of neutral) when the foot was 10-deg inverted ($p < 0.0001$) (Table 1). The average axial moment was internal at the neutral position and decreased by 1.39 Nm (515% of neutral) becoming external for

the 10-deg everted angle and increased by 1.05 Nm (389% of neutral) becoming more internal for the 10-deg inverted angle (Table 2). The polynomial decomposition indicated that both dependent variables responded linearly to the foot angle ($p < 0.0001$). The angular locations of the peak internal axial moment occurred near 30 deg and were not affected by the foot angle ($p = 0.7268$) (Table 1).

The change in the contribution of the moment due to the Fz component of the pedal force Mx′(Fz), was primarily responsible for the decrease in the varus knee moment as the foot was everted (Fig. 4). This subcomponent was valgus and increased as the foot was everted thus reducing the overall varus moment. Similar to the varus/valgus knee moment, the change in the contribution of the moment due to the Fz component of the pedal force Mz′(Fz) was primarily responsible for the decrease in the internal axial moment as the foot was everted (Fig. 4). The contribution of this subcomponent to the axial moment was external and increased substantially in the 10-deg everted position. Also the contribution

Fig. 3 Sample nondriving knee moments for one subject (subject 10) at the neutral (0), 10 degrees inverted (+10), and 10 deg everted (−10) foot angles. The varus (+Mx′)/valgus (−Mx′) and internal (+Mz′)/external (−Mz′) axial moments are expressed as net moments applied to the tibia.

Fig. 4 Contributions of individual pedal loads to the varus/valgus (Mx′) and internal/external axial (Mz′) knee moments for subject 10. Contributions are grouped by the inversion/eversion treatments, neutral ("0") and 10-deg everted ("−10"). Only the major contributors to each load component are plotted.
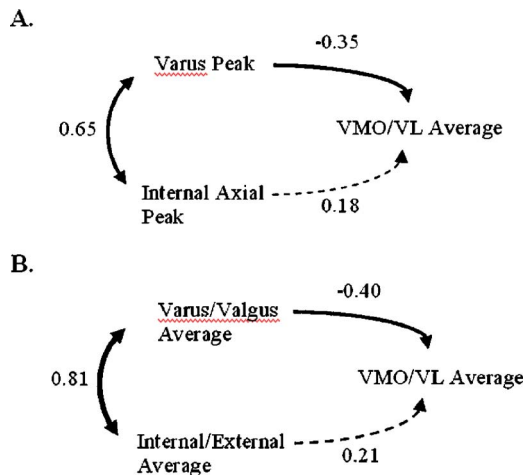
Table 3 Correlation coefficients (*r* values) between muscle activity variables and nondriving knee moment variables (15 subjects for VMO/VL ratio, 9 subjects for TFL), where subject effects were removed (*p* values in parentheses).

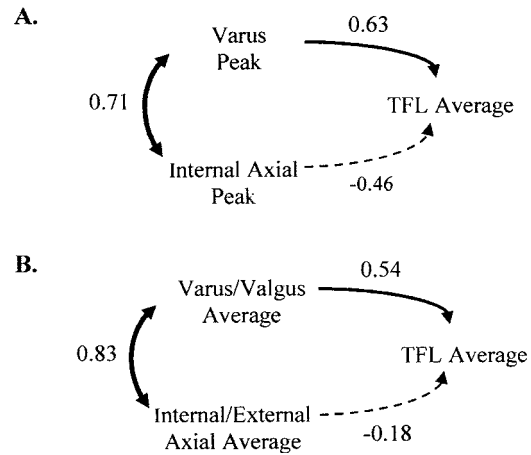|	VMO/VL ratio		TFL	
	Peak	Average	Peak	Average
Peak				
Varus	−0.10 (0.3863)	−0.23 (0.0434)	0.16 (0.2992)	0.30 (0.0462)
Internal Axial	0.09 (0.4340)	−0.05 (0.6768)	−0.038 (0.8065)	−0.013 (0.9338)
Average				
Varus/Valgus	−0.11 (0.3217)	−0.23 (0.0465)	0.23 (0.1370)	0.39 (0.0074)
Internal/External Axial	0.01 (0.9600)	−0.11 (0.3448)	0.19 (0.2050)	0.27 (0.0676)

of the Fx component of the pedal force to the axial moment Mz′(Fx) became external in the 10-deg everted position.

Nondriving Moments and Muscle Activation. For the sample of subjects, the percent difference in the average VMO/VL ratio was significantly correlated to both the peak varus moment ($r=-0.23, p=0.043$) and the average varus-valgus moment ($r=-0.23, p=0.046$) (Table 3). The negative sign of the *r* values indicates that the peak VMO activation increased relative to that of the VL as the varus moment decreased (foot everted).

The path analysis results indicated that the varus/valgus and axial knee moment quantities were significantly correlated (*r* values of 0.65 and 0.81 for peak and averages, respectively, $p < 0.0001$) and that the varus/valgus moment was the primary contributor to the relationships between the moment quantities and the average VMO/VL ratio (Fig. 5). The average standardized regression coefficient between the varus/valgus moment quantities and average VMO/VL ratio was −0.375 whereas the average standardized regression coefficient between the axial moment quanti-

Fig. 5 Path analysis results of the relative contributions by each of the nondriving knee moments to the correlation values in Table 3 for the VMO/VL ratio. (*a*) average VMO/VL ratio to varus and internal axial peaks, and (*b*) average VMO/VL ratio to varus/valgus and internal/external axial averages. The weights of the lines indicate the relative strength of the correlation (*r* values) between quantities presented. The *r* value between moment quantities is the correlation coefficient $\rho(x_1, x_2)$ and the *r* values between moment quantities and muscle quantities are the standardized regression coefficients b_1 and b_2. The *r* values between moment quantities were highly significant ($p < 0.0001$). See text for further explanation.

Fig. 6 Path analysis results of the relative contributions by the nondriving knee moments to the correlation values in Table 3 for the TFL activity. (*a*) TFL average to varus and internal axial peaks, and (*b*) TFL average to varus/valgus and internal/external axial averages. The weights of the lines represent the relative strength of the correlation (*r* values) between quantities presented. The *r* value between moment quantities is the correlation coefficient $\rho(x_1, x_2)$ and the *r* values between moment quantities and muscle quantities are the standardized regression coefficients b_1 and b_2. The *r* values between moment quantities were highly significant ($p < 0.0001$). See text for further explanation.

ties and average VMO/VL ratio was only 0.195 (Fig. 5).

For the nine subjects with usable TFL records, the average TFL activation was significantly correlated to both the peak varus moment ($r=0.30, p=0.046$) and the average varus/valgus moment ($r=0.39, p=0.007$) (Table 3). The positive sign of these two correlations indicates that the relative activation of the TFL decreased as the peak varus moment and average varus/valgus moment decreased (foot everted). The path analysis results indicated that these correlations were largely driven by the varus/valgus moment, rather than the internal/external axial moment (Fig. 6).

Discussion

Because patellofemoral pain syndrome is common in cycling and because non-driving intersegmental knee moment components are thought to be primarily responsible for the etiology of this injury by causing muscular imbalances, the objectives of this study were to examine the effects of changing the inversion/eversion foot angle on nondriving knee moments and to relate changes in the nondriving knee moments to the activation patterns of the VMO, VL, and TFL muscles. Two key findings of this study were that eversion of the foot decreased both the varus moment and the internal axial moment developed during the power stroke. Two other key findings were that a decrease in the varus moment was accompanied by an increase in the VMO/VL ratio and a decrease in the TFL activation.

Importance/Interpretation of Results. The result that everting the foot reduced the varus knee moment during the power stroke was expected. A trend toward decreasing varus knee moments as subjects exhibited greater overall forefoot angles (angle of intersecting forefoot and horizontal planes) has been observed previously [15]. Also everting the foot by means of specially designed footwear significantly reduced the varus knee moment in walking [36,37]. Because an anatomically inverted forefoot would have to evert to mate with the pedal platform, physically everting the foot to mate with the pedal platform was expected to likewise decrease the varus knee moment. The mechanism behind this decrease was that an everted foot angle caused the knee to travel in a more

medial position (closer to the sagittal plane of the bicycle) relative to the neutral foot position. The more medially located knee joint center increased the valgus moment arm of the Fz component of the pedal force thus increasing the valgus contribution of the $Mx'(Fz)$ subcomponent (Fig. 4). The average medial shift of the knee joint center from the neutral position due the 10-deg everted position was 2.77 cm during the power stroke for the 15 subjects ($p<0.0001$). The shift was systematic, where the path of the knee joint center in the frontal plane was not noticeably altered, which is consistent with the results of Sanderson et al. [38].

The result that the internal axial moment decreased during the power stroke was also expected, yet the mechanism was not. An applied varus moment to the shank causes coupled external axial rotation at the knee and an applied valgus moment causes coupled internal axial rotation at the knee [22]. Accordingly reducing the varus moment should reduce the amount of external axial rotation. Because of the constraint on foot abduction/adduction by the pedals which fixed the foot rigidly without allowing relative motion (i.e., float), external axial rotation was expected to manifest as an internal axial moment applied to the shank. Therefore, reducing the varus knee moment was expected to reduce the internal axial knee moment, which was the observed result. However, when examining the decomposition results (Fig. 4), the contribution of the axial pedal moment to the axial knee moment $Mz'(Mz)$ did not have a major effect on the axial knee moment. Rather, the medially shifted knee joint center for the everted position caused an increase in the external axial moment arm particularly for the Fz component of the pedal force thus increasing the external axial contribution of the $Mz'(Fz)$ subcomponent.

An interesting observation from the decomposition analysis is that neither of the moments developed at the pedal per se was an important contributor to the corresponding knee moment (Fig. 4). This observation has been made previously [39], leading to the conclusion that analyses of pedal moments yield little insight into the nondriving intersegmental knee moments.

The correlation between the varus/valgus knee moment quantities and the percent change in the average VMO/VL ratio (Table 3) is sufficiently strong to support a cause-and-effect relationship between this nondriving knee moment and patellofemoral pain syndrome. Although the values of the correlation coefficients imply that a large percentage of the variability was not accounted by a simple linear relationship, the values of the correlation coefficients indicate a biomechanical effect on the VMO/VL ratio. Because the correlation coefficient indicates the slope of a simple linear regression between variables with subject effects (i.e., means) removed, the strength of this effect can be appreciated based on relative changes indicated by the slopes. For example, the slope of the two significant correlations between the varus/valgus quantities and the percent change in the average VMO/VL ratio was -0.23. Thus decreasing the varus/valgus quantities by 35%, which was the decrease in the peak varus moment for a 5-deg everted position relative to the neutral position (Table 1), would result in a corresponding 8% increase in the VMO/VL ratio for these subjects. While it is unknown how large of an increase in the VMO/VL ratio would be necessary to either prevent or ameliorate patellofemoral pain syndrome, increases of this magnitude could positively benefit individuals either predisposed to, or suffering from, patellofemoral pain.

Furthermore, the path analysis results indicated that the varus/valgus moment has a stronger relation to the muscle activation than the axial moment (Fig. 5). Because the varus moment decreased when the foot was everted and the VMO/VL ratio increased (i.e., negative correlation), the relationship between this moment and the VMO/VL ratio is beneficial in that everting the foot should reduce lateral patellar tracking, hence reducing the potential for patellofemoral pain syndrome. This result is consistent with VMO strengthening studies, where hip adduction exercises caused increased VMO activity relative to the VL [40,41].

Because a significant relationship between the VMO/VL ratio

and the nondriving knee moments was evident for only two of the eight correlations studied, there may be either important subject-specific differences or methodological factors that could affect this relationship. One obvious subject-specific difference is in the anatomy of the lower limb. It has been argued that lower limb anatomy is related to both kinetic and kinematic variables of human movement. [15,42–44] Because there may be important subject-specific differences and/or methodological factors that affect the VMO/VL ratio, it would be advisable to assess the effectiveness of changing the inversion/eversion foot angle on a subject-by-subject basis.

The result that the varus/valgus knee moment decreased as the foot was everted and the TFL activation decreased (i.e., positive correlation, Table 3) complements the relationship between this moment and the VMO/VL ratio results. The relationship between this moment and the TFL activation is beneficial in that everting the foot should further reduce lateral patellar tracking.

Methodological Issues. Because factors affecting the computations of the nondriving knee moments have been discussed previously [16], this discussion will be only summarized here. First, the coordinate system chosen to express knee loads was based on the desire to reflect functionally and clinically meaningful directions, while remaining orthogonal. Second, there are two primary sources of error in the computation of the knee joint loads, error inherent to the motion analysis system and skin movement. Because motion analysis errors are composed of random, high frequency components, [45], the low-pass digital filtering operation as well as averaging of the data over multiple crank cycles reduced errors of this type. Because only two markers used in this study were prone to skin movement artifacts and because skin motion produced systematic errors in the load calculations, skin movement errors did not substantively affect the relative changes in the nondriving knee load computations, which were of primary interest in this study.

An assumption implicit to the preceding discussion regarding the potential effect of changes in muscle activity on patellofemoral pain syndrome is that relative changes in muscle activation indicate corresponding relative changes in muscle force. The prediction of muscle force from EMG records has been examined extensively and the general consensus is that force cannot be predicted with reasonable accuracy for non-isometric contractions (reviewed in [7,46,47]). The complex combination of recruitment, rate coding, muscle architecture, muscle fiber type, and force-length-velocity properties determines the force generated by muscle. In addition, the use of surface electrodes in nonisometric contractions is problematic because the electrodes record action potentials from different locations along the muscle during a contraction. These factors constitute a highly complex, nonlinear relationship which makes the accurate determination of absolute muscle force from EMG highly unlikely.

Notwithstanding the conclusion that absolute muscle force cannot be predicted from EMG during dynamic contractions, the assumption that relative changes in muscle activation indicate relative changes in muscle force was justified. First, muscle architecture and fiber type properties did not change during the course of an experiment and hence were constant. Second, the treatments did not alter the pedaling kinematics substantively so that the force-length-velocity relationships for the muscles did not vary across treatments. Third, motor unit recruitment is the primary mechanism for increasing force output for muscles with high innervation ratios [7], so that rate coding was constant in the muscles examined. Last, all electrodes remained in place over the duration of the study and each subject served as his own control. Consequently, the only property that changed was motor unit recruitment, which is proportional to both muscle force and activation as indicated by the processed EMG. Therefore relative changes in the activation reflected relative changes in muscle force.

Because the gluteus maximus also inserts on the iliotibial band,

recordings of this muscle might also have been useful to examine the hypothesis that reduction in the activity of muscles inserting on the iliotibial band decreases the potential for lateral patellar tracking. Because of its lateral location and large valgus moment arm however, recordings of the TFL were expected to yield higher resolution of the inversion/eversion treatment effects on the activity of muscles inserting on the iliotibial band than the gluteus maximus.

In summary, everting the foot could reduce the potential for patellofemoral pain syndrome in the cycling population. This reduction occurs because eversion reduced nondriving knee moments while the VMO/VL ratio increased and the TFL activation decreased. Both of these changes in muscle activation potentially reduce lateral patellar tracking thus decreasing the risk of injury to the patellofemoral joint. For the benefits of everting the feet to be demonstrated conclusively, it would be worthwhile to test subjects who suffer from patellofemoral pain syndrome using pedals which evert the feet to determine whether they gain any relief.

Acknowledgment

References

[1] Holmes, J. C., Pruitt, A. L., and Whalen, N. J., 1991, "Cycling Knee Injuries," Cycling Science, **3**, pp. 11–14.

[2] Weiss, B. D., 1985, "Nontraumatic Injuries in Amateur Long Distance Bicyclists," Am. J. Sports Med., **13**, pp. 187–192.

[3] Wilber, C. A., Holland, G. J., Madison, R. E., and Loy, S. F., 1995, "An Epidemiological Analysis of Overuse Injuries among Recreational Cyclists," Int. J. Sports Med., **16**, pp. 201–206.

[4] Goodfellow, J., Hungerford, D. S., and Woods, C., 1976, "Patello-Femoral Joint Mechanics and Pathology. 2. Chondromalacia Patellae," J. Bone Jt. Surg., Br. Vol., **58**, pp. 291–299.

[5] Insall, J., 1982, "Current Concepts Review: Patellar Pain," J. Bone Jt. Surg., Am. Vol., **64**, pp. 147–152.

[6] Lieb, F. J., and Perry, J., 1968, "Quadriceps Function. An Anatomical and Mechanical Study Using Amputated Limbs," J. Bone Jt. Surg., Am. Vol., **50**, pp. 1535–1548.

[7] Basmajian, J. V., and De Luca, C. J., 1985, *Muscles Alive: Their Functions Revealed by Electromyography*, Williams & Wilkins, Baltimore, MD.

[8] Ericson, M. O., and Nisell, R., 1987, "Patellofemoral Joint Forces During Ergometric Cycling," Phys. Ther., **67**, pp. 1365–1369.

[9] Pruitt, A. L., 1988, "The Cyclist's Knee: Anatomical and Biomechanical Considerations," *Medical and Scientific Aspects of Cycling*, E. R. Burke and M. M. Newsoms, eds., Human Kinetics, Champaign, IL, pp. 16–24.

[10] Huberti, H. H., and Hayes, W. C., 1984, "Patellofemoral Contact Pressures. The Influence of Q-Angle and Tendofemoral Contact," J. Bone Jt. Surg., Am. Vol., **66**, pp. 715–724.

[11] Sanner, W. H., and O'Halloran, W. D., 2000, "The Biomechanics, Etiology, and Treatment of Cycling Injuries," J. Am. Podiatr. Med. Assoc., **90**, pp. 354–376.

[12] Wolchok, J. C., Hull, M. L., and Howell, S. M., 1998, "The Effect of Intersegmental Knee Moments on Patellofemoral Contact Mechanics in Cycling," J. Biomech., **31**, pp. 677–683.

[13] Boyd, T. F., Neptune, R. R., and Hull, M. L., 1997, "Pedal and Knee Loads Using a Multi-Degree-of-Freedom Pedal Platform in Cycling," J. Biomech., **30**, pp. 505–511.

[14] Ruby, P., Hull, M. L., and Hawkins, D., 1992, "Three-Dimensional Knee Joint Loading During Seated Cycling," J. Biomech., **25**, pp. 41–53.

[15] Ruby, P., Hull, M. L., Kirby, K. A., and Jenkins, D. W., 1992, "The Effect of Lower-Limb Anatomy on Knee Loads During Seated Cycling," J. Biomech., **25**, pp. 1195–1207.

[16] Gregersen, C. S., and Hull, M. L., 2003, "Non-Driving Intersegmental Knee Moments in Cycling Computed Using a Model That Includes Three-Dimensional Kinematics of the Shank/Foot and the Effect of Simplifying Assumptions," J. Biomech., **36**, pp. 803–813.

[17] Buchanan, T. S., Kim, A. W., and Lloyd, D. G., 1996, "Selective Muscle Activation Following Rapid Varus/Valgus Perturbations at the Knee," Med. Sci. Sports Exercise, **28**, pp. 870–876.

[18] Buchanan, T. S., and Lloyd, D. G., 1997, "Muscle Activation at the Human Knee During Isometric Flexion-Extension and Varus-Valgus Loads," J. Orthop. Res., **15**, pp. 11–17.

[19] Fulkerson, J. P., Hungerford, D. S., and Ficat, P., 1990, *Disorders of the Patello-Femoral Joint*, Williams & Wilkins, Baltimore, MD.

[20] Puniello, M. S., 1993, "Iliotibial Band Tightness and Medial Patellar Glide in Patients with Patellofemoral Dysfunction," J. Orthop. Sports Phys. Ther., **17**, pp. 144–148.

[21] Kwak, S. D., Ahmad, C. S., Gardner, T. R., Grelsamer, R. P., Henry, J. H., Blankevoort, L., Ateshian, G. A., and Mow, V. C., 2000, "Hamstrings and Iliotibial Band Forces Affect Knee Kinematics and Contact Pattern," J. Orthop. Res., **18**, pp. 101–108.

[22] Mills, O. S., and Hull, M. L., 1991, "Rotational Flexibility of the Human Knee Due to Varus/Valgus and Axial Moments in Vivo," J. Biomech., **24**, pp. 673–690.

[23] Blankevoort, L., Huiskes, R., and deLange, A., 1988, "The Envelope of Passive Knee Joint Motion," J. Biomech., **21**, pp. 705–720.

[24] Andrews, J. G., 1995, "Euler's and Lagrange's Equations for Linked Rigid-Body Models of Three-Dimensional Human Motion," in *Three-Dimensional Analysis of Human Movement*, P. Allard, I. Stokes, and J. Blanchis, eds., Human Kinetics, Champaign, IL, pp. 145–175.

[25] de Leva, P., 1996, "Adjustments to Zatsiorsky-Seluyanov's Segment Inertia Parameters," J. Biomech., **29**, pp. 1223–1230.

[26] Ruby, P., and Hull, M. L., 1993, "Response of Intersegmental Knee Loads to Foot/Pedal Platform Degrees of Freedom in Cycling," J. Biomech., **26**, pp. 1327–1340.

[27] Hollister, A. M., Jatana, S., Singh, A. K., Sullivan, W. W., and Lupichuk, A. G., 1993, "The Axes of Rotation of the Knee," Clin. Orthop. Relat. Res., **290**, pp. 259–268.

[28] Delagi, E. F., Perotto, A., Iazzetti, J., and Morrison, D., 1975, *Anatomic Guide for the Electromyographer*, Charles C. Thomas, Springfield, IL.

[29] Winter, D. A., 1990, *Biomechanics and Motor Control of Human Movement*, Wiley, New York.

[30] Zajac, F. E., 1989, "Muscle and Tendon: Properties, Models, Scaling, and Application to Biomechanics and Motor Control," Crit. Rev. Biomed. Eng., **17**, pp. 359–411.

[31] Raasch, C. C., Zajac, F. E., Ma, B., and Levine, W. S., 1997, "Muscle Coordination of Maximum-Speed Pedaling," J. Biomech., **30**, pp. 595–602.

[32] Winters, J. M., and Stark, L., 1988, "Estimated Mechanical Properties of Synergistic Muscles Involved in Movements of a Variety of Human Joints," J. Biomech., **21**, pp. 1027–1041.

[33] Neptune, R. R., Kautz, S. A., and Hull, M. L., 1997, "The Effect of Pedaling Rate on Coordination in Cycling," J. Biomech., **30**, pp. 1051–1058.

[34] Huynh, H., and Feldt, L. S., 1976, "Estimation of the Box Correction for Degrees of Freedom from Sample Data in Randomized Block and Split-Plot Designs," J. Educ. Stat., **1**, pp. 69–82.

[35] Li, C. C., 1975, *Path Analysis: A Primer*, Boxwood Press, Pacific Grove, CA.

[36] Kerrigan, D. C., Lelas, J. L., Goggins, J., Merriman, G. J., Kaplan, R. J., and Felson, D. T., 2002, "Effectiveness of a Lateral-Wedge Insole on Knee Varus Torque in Patients with Knee Osteoarthritis," Arch. Phys. Med. Rehabil., **83**, pp. 889–893.

[37] Fisher, D., Andriacchi, T., Alexander, E., Dyrby, C., and Morag, E., 2005, "Initial Gait Characteristics Influence the Effect of Footwear Intervention to Modify Knee Loading," Transactions of the Orthopedic Research Society.

[38] Sanderson, D. J., Black, A. H., and Montgomery, J., 1994, "The Effect of Varus and Valgus Wedges on Coronal Plane Knee Motion During Steady-Rate Cycling," Clin. J. Sport Med., **4**, pp. 120–124.

[39] Hull, M. L., and Ruby, P., 1996, "Preventing Overuse Knee Injuries," in *High-Tech Cycling*, E. R. Burkes, ed., Human Kinetics, Champaign, IL, pp. 251–279.

[40] Hodges, P. W., and Richardson, C. A., 1993, "The Influence of Isometric Hip Adduction on Quadriceps Femoris Activity," Scand. J. Rehabil. Med., **25**, pp. 57–62.

[41] Hanten, W. P., and Schulthies, S. S., 1990, "Exercise Effect on Electromyographic Activity of the Vastus Medialis Oblique and Vastus Lateralis Muscles," Phys. Ther., **70**, pp. 561–565.

[42] Cavanagh, P. R., Morag, E., Boulton, A. J., Young, M. J., Deffner, K. T., and Pammer, S. E., 1997, "The Relationship of Static Foot Structure to Dynamic Foot Function," J. Biomech., **30**, pp. 243–250.

[43] McPoil, T. G., and Cornwall, M. W., 1996, "The Relationship between Static Lower Extremity Measurements and Rearfoot Motion During Walking," J. Orthop. Sports Phys. Ther., **24**, pp. 309–314.

[44] Nigg, B. M., Cole, G. K., and Nachbauer, W., 1993, "Effects of Arch Height of the Foot on Angular Motion of the Lower Extremities in Running," J. Biomech., **26**, pp. 909–916.

[45] Cappozzo, A., 1991, "Three-Dimensional Analysis of Human Walking: Experimental Methods and Associated Artifacts," Hum. Mov. Sci., **10**, pp. 589–602.

[46] Hof, A. L., 1984, "Electromyography and Muscle Force: An Introduction," Hum. Mov. Sci., **3**, pp. 119–153.

[47] Perry, J., and Bekey, G. A., 1981, "EMG-Force Relationships in Skeletal Muscle," Crit. Rev. Biomed. Eng., **7**, pp. 1–22.